Exp Biomed Res 2022; 5(1): 58-72
Doi: 10.30714/j-ebr.2022173851

Experimental Biomedical Research **Original article**

The variation of 5'-carboxycytosine localization within the nucleus of normal and cancerous cells

Selcen Celik Uzuner

Department of Molecular Biology and Genetics, Faculty of Science, Karadeniz Technical University, Trabzon, Turkey

ABSTRACT

Aim: Cytosine modifications are the common epigenetic marks during cellular processes. The pattern of cytosine modifications varies depending on the tissues and the developmental stages. The interactions within the epigenome are complex, and co-existence of cytosine modifications provides understanding on their collaborative or distinct functions. This study aims to disclose the intra-nuclear co-location of 5'-carboxycytosine with other modified cytosine bases in normal and cancerous cells.

Methods: Co-localization patterns were assessed using an immunostaining protocol enhanced with enzyme treatments, and microscope images were analyzed using Image J co-localization plug in.

Results: Findings showed that most of 5'-carboxycytosine is associated with oxidized forms of 5'-methylcytosine; however, some extent of individual localization was detected following different antigen retrievals.

Conclusion: These suggest that antigenicity reveals variation in the detection of the co-existence of cytosine modifications. The spatial organization of chromatin may be expected to affect this variation and it needs further investigation.

Key words: Epigenetics, cytosine modifications, immunofluorescence, co-localization, cancer.

✉ *Selcen Celik Uzuner*
Department of Molecular Biology and Genetics, Faculty of Science, Karadeniz Technical University, Trabzon, Turkey
E- mail: selcen.celik@ktu.edu.tr
Received: 2021-07-10 / Revisions: 2021-10-19
Accepted: 2021-10-24 / Published online: 2022-01-01

Introduction

Epigenetic mechanisms are involved in the regulation of gene expression. The mechanisms include reversible chemical modifications of histone proteins and DNA. DNA methylation occurring on cytosine bases (5'-methylcytosine, 5meC or 5mC) is a well-described modification. DNA methylation has been shown to be associated with gene regulation in development and alterations in its pattern were found in different diseases, such cancer and neurodegenerative diseases [1-3]. The pattern of epigenetic mechanisms is highly dynamic depending on the cellular processes. For instance, methyl groups have been supposed to be removed from methylated cytosines during the preparations for DNA repair machinery, and the methylation mark has been erased gradually by the conversion of methyl to other chemical groups, such hydroxyl and formyl [4, 5]. These oxidized forms of cytosine methylation including hydroxymethylation (5hmC), formulation (5fC) and carboxylation (5caC) catalyzed by Ten-Eleven-Translocation (TET) enzymes, are supposed to be intermediates of active demethylation process in particular during DNA repair [6-8]. Additionally, there is

an increasing evidence revealing the potential function of these modifications in the regulation of gene expression as well [9-11]. The patterns of cytosine modifications have been found to change in tissue-specific manner and also during different steps of development [12-18]. The findings that show the patterns of cytosine modifications are likely associated with disease progresses support their biological significance.

Immunofluorescence is a powerful tool to reveal both quantitative and qualitative profile of cytosine modifications. The spatial organization of modifications within the nuclei can be assessed, and co-existence patterns of modifications are also evaluated by fluorescence-based microscopies. This provides understanding whether there are complex interactions between modifications suggesting their co-function during cellular processes. This study aimed to reveal the co-localization of 5'-carboxycytosine (5caC) with 5meC, 5hmC and 5fC in cancer and normal cells using the newly developed immunofluorescence protocol with different antigen retrieval approaches. Antigen retrieval is one of the most important steps in immunostaining of DNA epitopes as it utilizes the accessibility of DNA epitopes (*i.e*. cytosine modifications) to be labelled by the specific antibodies. The usual application for antigen retrieval is acid treatment; however previous studies showed that acid treatment alone did not unmask some extent of methylated cytosines and also other modifications from protein content [19-22]. The protocol was enhanced with the additional use of trypsin and pepsin enzymes that have different proteolytic activities [19, 20]. The sequential treatment of cells with acid, trypsin and pepsin revealed increased amounts of staining in each modification. But amount of the epigenetic marks is not the only parameter that is supposed to be altered after methodological improvements. This study aims to disclose the intra-nuclear co-location of 5'-carboxycytosine with other modified cytosine bases in normal and cancerous cells. In this study, the new immunostaining protocol further showed that a majority of 5caC (more than 70%) was co-localized with 5meC, 5hmC or 5fC in the cells. But antigen retrievals with additional enzyme treatments provided a significant amount of 5caC that independently localized from cytosine methylation in normal cells. The co-existence pattern of 5caC with 5fC was not affected using acid and/or enzymes in normal cells, whereas it was significantly changed after the treatments with enzymes in both cancer cells. Therefore, 5caC's localization within the nucleus highly depends on solvent-exposure of regions of carboxymethylated cytosines in cells, and the detection of immune-localization of DNA modifications is highly associated with three-dimensional structure of chromatin-DNA complex that is organized within the chromatin layers with different response to enzymatic reactions. These findings suggest that classical immunofluorescence protocol with acid use alone can likely overestimate the co-localization of 5caC with other cytosine modifications depending on the cell type. Therefore, technical limitation can prevent the detection of 5caC that is separately located within the cell nucleus.

Materials and methods

Cell culture

CF-1 embryonic fibroblasts (American Type Cell Collection ATCC, Cat No SCRC-1040, VA, US), AR42J pancreatic cancer cells (ATCC, Cat No CRL-1492) and HeLa cervical cancer cells (ATCC, Cat No CCl-2) were used. Cells were cultured in DMEM (Wisent Inc., Cat

No 319-005-CL, Quebec, Canada), RPMI (Wisent, Cat No 350-000-CL) or in EMEM (Wisent, Cat No 320-026-CL), respectively. Complete media included 10% of foetal bovine serum (FBS) (Capricorn Scientific GmbH, Cat No FBS11-A, Ebsdorfergrund, Germany) and 1% streptomycin-penicillin (Wisent, Cat No 450-201-EL), and cells were cultured in chamber slides (Ibidi GmbH, Cat No 81201, Martinsried, Germany) at 37°C with 5% CO_2.

Immunostaining protocol

Cells were fixed and stained as described previously [20]. The protocol briefly included permeabilization of fixed cells, antigen retrieval, and incubations with primary and secondary antibodies. Antigen retrieval (AR) process included 4N hydrochloric acid (Merck KGaA, Cat No 100319, Darmstadt, Germany) alone or 0.25% trypsin-EDTA (Wisent, Cat No 325-043-EL) after acid or acid followed by 0.25% trypsin-EDTA and pepsin (Sigma Aldrich Co., Cat No P7000, St. Louis, USA). Acid was treated for 10 min at room temperature (RT), and enzymes were treated for 1 min at 37°C. Pepsin concentrations used were 0.1 mg/ml, 0.5 mg/ml or 1 mg/ml as these conditions were defined for each cell in the previous study [20]. The applied pepsin conditions for AR step are summarized in Table 1.

Table 1. Pepsin concentrations applied after acid and trypsin for each co-localization in cells.

Cell	Co-localization		
	5caC and 5meC (mg/ml)	5caC and 5hmC (mg/ml)	5caC and 5fC (mg/ml)
CF-1	0.1	0.1	1
AR42J	0.1	0.1	0.1
HeLa	N/A	1	1

After pepsin treatment, cells were washed with 1xPBS (phosphate-buffered saline) (Biomatik, Cat No A3602, Ontario, Canada) for 3 times. Cells were blocked with 50 % goat serum at 4°C overnight followed by the treatment with primary antibodies for 1) anti-5meC (mouse anti-5meC; Active Motif Inc. Cat No 39649, Carlsbad, CA) at 1:400 for 1 h at RT, 2) anti-5hmC (rabbit anti-5hmC; Active Motif Cat No 39791) at 1:1000 overnight at 4°C, 3) anti-5fC (rabbit anti-5fC; Active Motif Cat No 61223) at 1:1000 overnight at 4°C and/or 4) anti-5caC (rabbit anti-5caC; Active Motif Cat No 61225) at 1:1000 overnight at 4°C. Primary antibodies were washed with 1xPBS followed by incubations with secondary antibodies (Alexa 488 mouse Abcam Cat No Ab150113, Cambridge, UK, Alexa 488 rabbit Abcam Cat No Ab150077 or Texas Red rabbit Abcam Cat No Ab6719). Secondary antibody conditions for each primary antibody were 1) 1 h at RT, 2) 1:1000 for 1 h at RT, 3) 1:1000 for 2 h at RT, and 4) 1:1000 4°C overnight, respectively. Cytosine methylation was also co-stained with MBD1 protein (methyl-binding protein-1) in mouse embryonic fibroblasts or with mitochondria in MDA-MB-231 cell line (ATCC, Cat No HTB-26). Anti-MBD1 antibody was purchased from Abcam (Cat No ab3753) and incubated at 4°C overnight after the treatment with anti-5meC antibody. MitoTracker Red CMXRos was purchased from ThermoFisher Scientific (Massachusetts, USA, Cat No M7512) and used at 400nM within the culture media for 45 min at 37°C. Cells then were fixed with 4% paraformaldehyde (w/v) (ChemSolute, Th. Geyer GmbH & Co., Cat No 8416-0500, and Germany) for half an hour at room temperature (RT), and visualized under the microscope. Non-immune IgG antibodies for rabbit (Abcam, Cat No ab172730) and mouse (Sigma,

Cat No I8765) were used to show negative staining. Representative green and red channel images after treatment with non-immune IgG are shown in Figure 1.

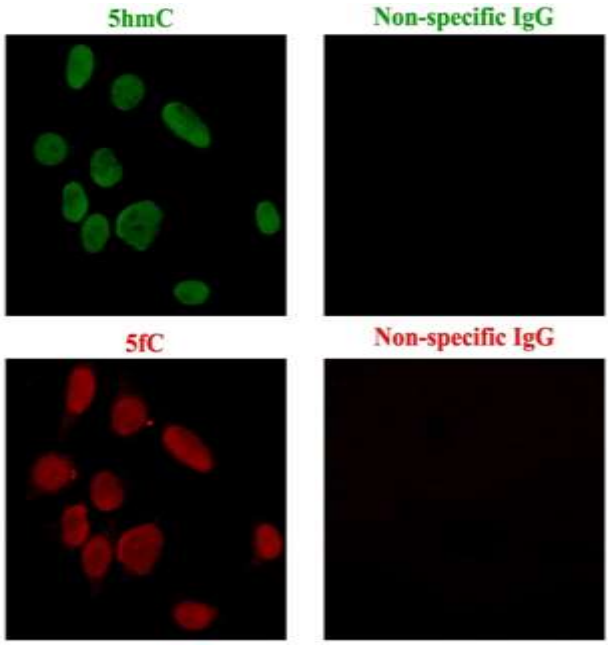

Figure 1. Representative non-specific IgG staining in parallel with 5hmC and 5fC staining in HeLa cells. Non-specific (non-immune IgG) treatment did not reveal any detectable staining both in green and red channels. Non-specific IgG control staining was included in each immunostaining in this study (not all data shown).

Co-localization analysis

Stained cells were visualized using a 40x objective of the inverted fluorescence microscope (AxioVert A1, Carl Zeiss, and Germany). Images were taken for both green and red filters. Images from both channels were analyzed using co-localization plug-in of Image J software (NIH, US). The steps for co-localization analysis briefly include i) subtraction of background, ii) conversion of both images to 8-bit grey scale, and iii) calculation of Mander's overlap coefficient using co-localization plug-in [23]. Co-existence of modifications was represented by Pearson's correlation coefficient, Mander's correlation (overlap) coefficient, M1 and M2 values. Pearson's correlation coefficient represents the correlation between the intensities of two signals (green and red in this study), and this is a value between -1 (negative correlation) and +1 (positive correlation). Mander's correlation coefficient indicates the co-localization level of two signals within the nuclei and this parameter is between 0 and 1. Values close to 1 indicate high co-localization. M1 and M2 values represent split-coefficients for red and green channels, respectively.

Statistical analysis

Statistical comparisons for co-localization coefficients, M1 and M2 values were performed using UNIANOVA (univariate analysis of variance) of SPPS software (Version 23). Significance levels used were $p<0.05$ (*), $p<0.01$ (**), $p<0.001$ (***) and $p<0.0001$ (****). Each experiment was performed as triplicates and standard errors of the mean (+/- s.e.m) were used to evaluate deviation of the calculations between independent repeats.

Results

Evaluation of co-localization of different epitopes

First of all, co-localization profiles were examined using nuclear (including 5meC, 5hmC, MBD1-methyl-binding protein 1) and/or extra-nuclear epitopes (a marker for mitochondria) in different cell lines to interpret the relationship between the co-localization coefficient values, the co-localization plot pattern and the actual co-staining. The representative co-localization patterns show co-localization plots of red (channel 1, X axes of co-localization plot) and green (channel 2, Y axes of co-localization plot) channels with co-localization coefficients from high to low (from up to down) (Figure 2A-F) and microscopy

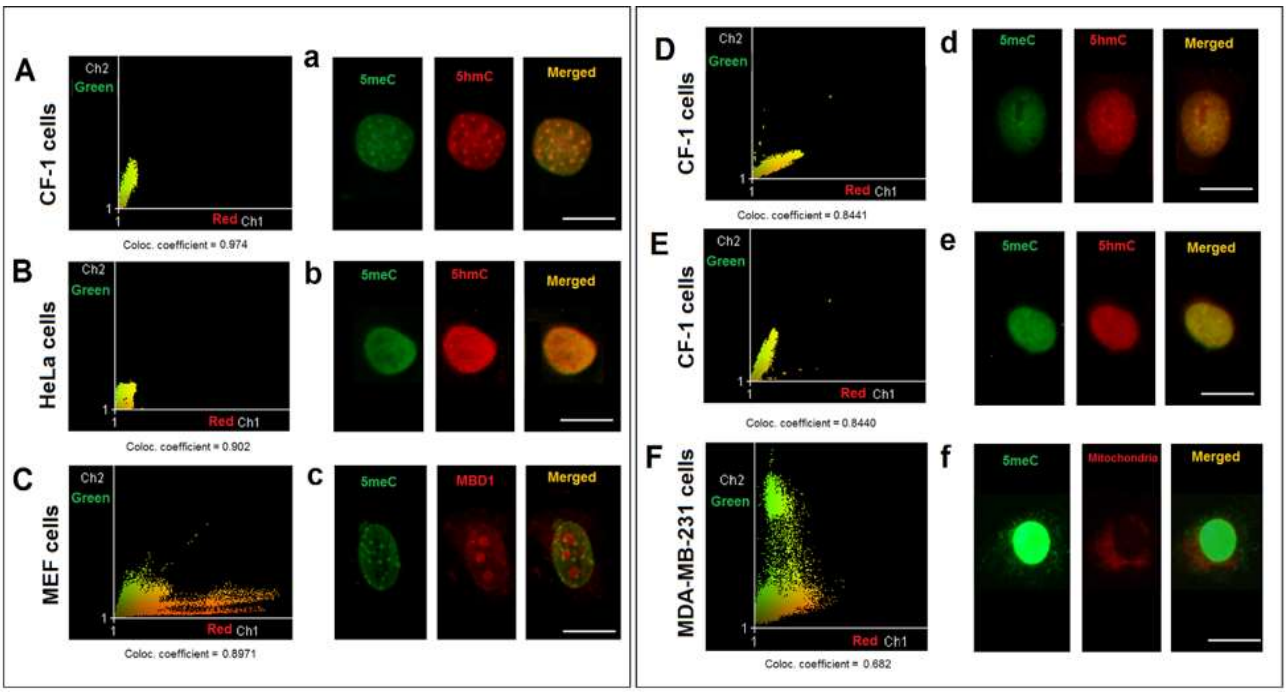

Figure 2. Examples of co-localisation profiles of two epitopes in different cell lines**. A, B, C, D, E** and **F** show the representative co-localisation plots for correlation coefficients from high to low, respectively. **a, b, c, d, e** and **f** show the representative microscopy images of individual and merged staining for **A, B, C, D, E** and **F**, respectively. **A (a)**, **D (d)** and **E (e)** show 5meC-5hmC co-staining in CF-1 cells, **B (b)** show 5meC-5hmC co-staining in HeLa cells, **C (c)** show 5meC-MBD1 co-staining in mouse embryonic fibroblasts (MEF), **F (f)** show 5meC-mitochondria co-staining in MDA-MB-231 cells. Scale bar is 10 micron.

images of nuclei at each channel together with the merged images for co-localization throughout the nucleus (Figure 2a-f). The close and high coefficient values (between 0.84 and 0.97) can indicate different co-localization than each other (Figure 2A-E). For instance, some of MBD1 protein localized as distinct large foci regions independently from DNA methylation (5meC) (Figure 2c) that was represented by a distinct population in red channel (Figure 2C). Similarly, some of 5meC existed within the small foci that were not co-localized with MBD1 (Figure 2c). But the general co-localization value of those two markers is around 0.9. Another example includes co-staining of 5meC with a mitochondrial marker for membrane permeability (Figure 2F, f). A large population of 5meC within the cells was not associated with mitochondrial staining as represented by a distinct population in green channel; however, there was a small yellowish region representing co-localization (Figure 2F). Co-localization coefficient of 5meC and mitochondria was around 0.7. The representatives suggest that the distribution of the existence of two markers within the plots can vary even if co-localization coefficients were close to each other. Besides, the plots and coefficients should be evaluated together with merged images to conclude about the co-existence profiles.

Co-localization of 5caC and 5meC

The majority of 5-carboxycytosine was found to be co-localized with DNA methylation (5meC) in both CF-1 and AR42J cells (Figure 3). In CF-1 normal fibroblast cells, the co-existence of 5caC and 5meC was decreased after enzyme use (p<0.001) in the antigen retrieval step (Figure 3A -C). This suggests that protein compounds which are acid-resistant but enzyme-sensitive can result in overestimation

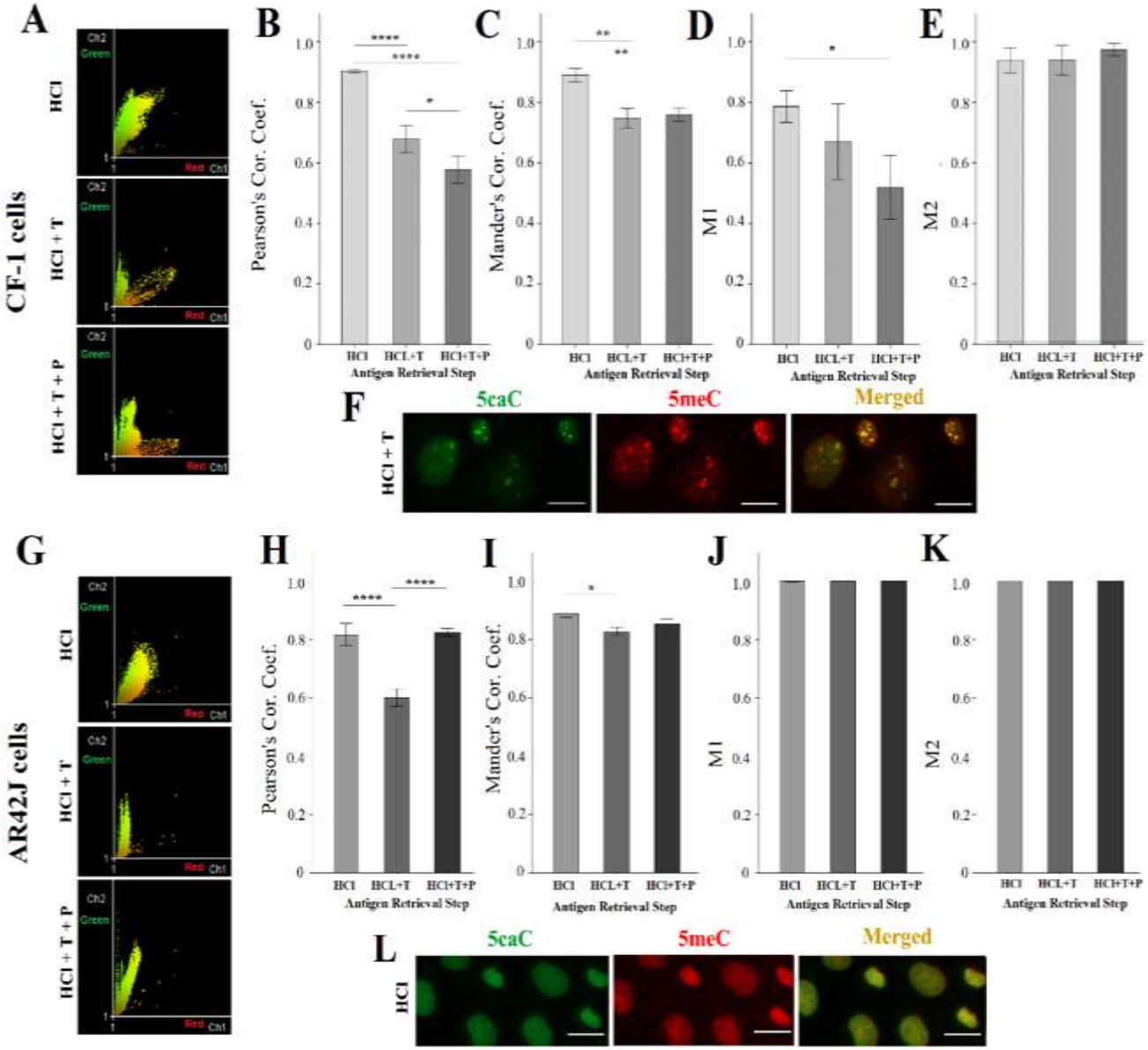

Figure 3. The co-localisation of 5caC and 5meC in CF-1 and AR42J cells. CF-1 cells **(A-F)** and AR42J **(G-L)** include co-localisation dot plots of 5caC (green) and 5meC (red) after acid alone (HCl), acid + trypsin (HCl + T) and acid + trypsin + pepsin (HCl + T + P) **(A, G)**, bar graphs for the comparisons of Pearson's correlation coefficients **(B, H)**, Mander's correlation coefficients **(C, I)**, M1 values **(D, J)**, M2 values **(E, K)** and representative microscopy images **(F, L)**. Bar graphs show +/- standard error of the mean of independent triplicates. Scale bar is 10 micron. $p<0.05$ (*), $p<0.01$ (**) and $p<0.0001$ (****)

of the co-localization degree of 5caC and 5meC. 68 % of 5meC was associated with 5caC and around 52 % of 5meC was significantly found to be independently from 5caC after sequential treatment of cells with acid, trypsin, and pepsin ($p<0.05$) (Figure 3D). However almost 90% of 5caC was localized with methylated regions (Figure 3E), and this pattern was not affected by the choice of antigen retrieval ($p>0.05$). Both 5caC and 5meC existed within distinct focal regions within the nuclei, and many of foci were stained for both (Figure 3F). In AR42J cancer cells, the co-localization value of 5caC with 5meC was above 0.8 after HCl alone or followed by trypsin and pepsin (Figure 3G, H). However, only trypsin treatment after acid resulted in a significant decrease in the detection of co-localized 5meC

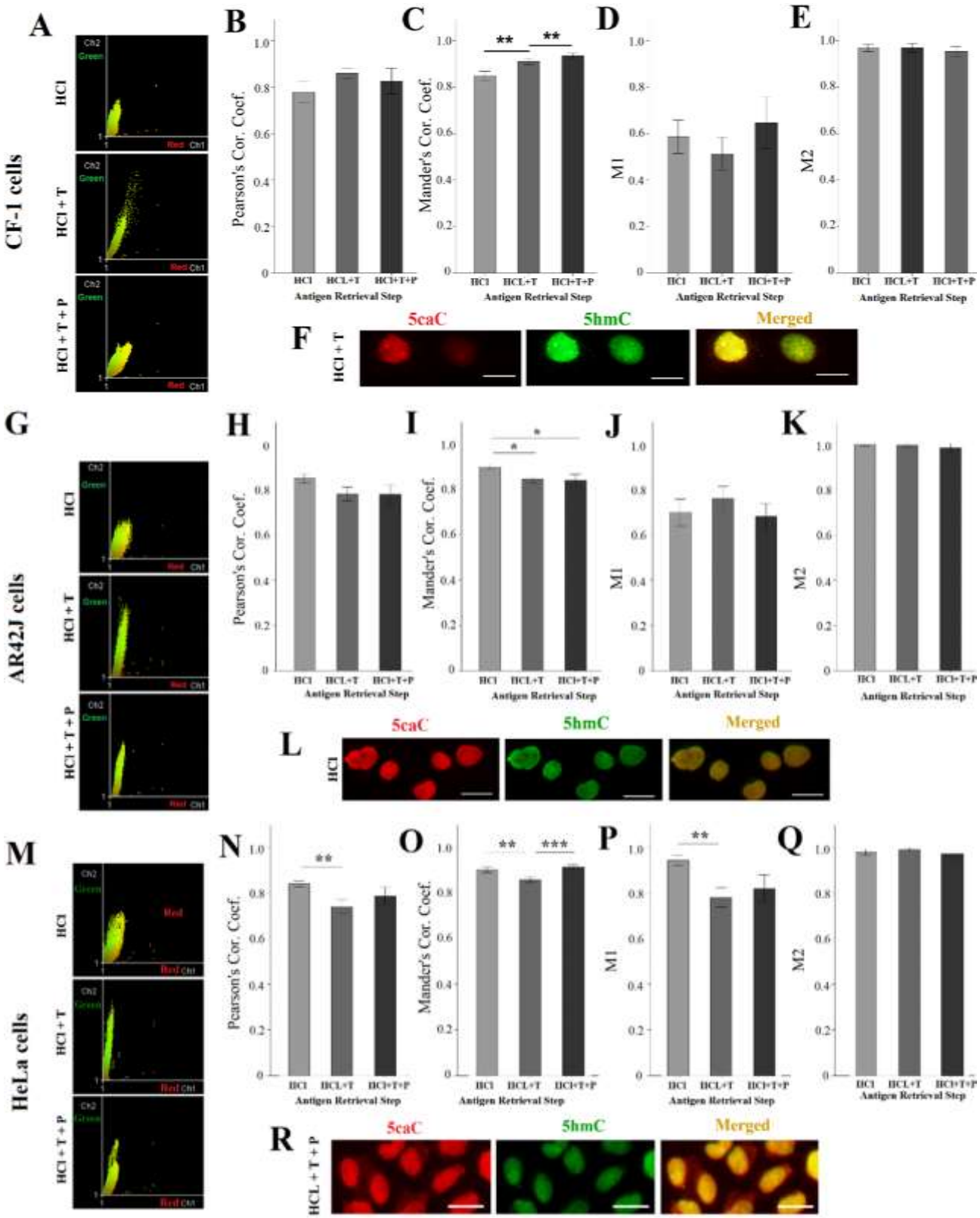

Figure 4. The co-localisation of 5caC and 5hmC in CF-1, AR42J and HeLa cells. CF-1 cells **(A-F),** AR42J **(G-L)** and HeLa cells **(M-R)** include co-localisation dot plots of 5caC (red) and 5hmC (green) after acid alone (HCl), acid + trypsin (HCl + T) and acid + trypsin + pepsin (HCl + T + P) **(A, G, M)**, bar graphs for the comparisons Pearson's correlation coefficients **(B, H, N)**, of Mander's correlation coefficients **(C, I, O)**, M1 values **(D, J, P)**, M2 values **(E, K, Q)** and representative microscopy images **(F, L, R)**. Bar graphs show +/- standard error of the mean of independent triplicates. Scale bar is 10 micron. $p<0.05$ (*), $p<0.01$ (**) and

and 5caC (Mander's correlation coefficient $p<0.05$, Pearson's correlation coefficient $p<0.0001$) (Figure 3H, I). Almost all 5meC's localization was associated with 5caC (Figure 3J), and all 5caC was co-localized with 5meC as well (Figure 3K). The use of enzymes did not result in a significant change in both M1 and M2 values ($p>0.05$). Differentially from CF-1 cells, most of both 5meC and 5caC diffusely localized within the nucleus (Figure 3L).

Co-localization of 5caC and 5hmC

In CF-1 mouse embryonic fibroblasts, there was no difference in Pearson's correlation between 5caC and 5hmC, whereas analysis of Mander's correlation coefficient showed that co-localization values were high (more than 0.85) and enzyme use improved the detection of co-existence of 5caC with 5hmC ($p<0.01$ for each) compared to acid treatment alone (Figure 4A,-C). However, antigen retrieval did not reveal a different pattern of M1 and M2 values (Figure 4D, E). Only half of the 5caC was co-localized with 5hmC (Figure 4D) but almost all 5hmC was found to be co-localized with 5caC (Figure 4E). 5caC and 5hmC were found within both diffuse and focal regions of nuclei (Figure 4F). In AR42J pancreatic cancer cells, Pearson's correlation was not different, Mander's co-localization values were more than 0.8, and each enzyme did reveal less co-localized pattern of 5caC and 5hmC ($p<0.05$ for each) (Figure 4G-I). But enzymes did not significantly affect M1 and M2 values as around 70% of 5caC were co-localized with 5hmC throughout the nucleus (Figure 4J). Almost all 5hmC (99%) was found together with 5caC (Figure 4K). Differentially from CF-1 cells, both modifications existed within the nucleus as diffuse pattern (Figure 4L). In HeLa cells, trypsin treatment after acid resulted with a decrease in the detection of co-localization ($p<0.01$ compared to acid alone, $p<0.001$ compared to enhanced retrieval with pepsin) similar to Pearson's correlation coefficient, but all applications for antigen retrieval indicate that the co-localization degree for 5caC and 5hmC was around 0.9 (Figure 4M-O). The M1 value was decreased after the additional treatment of acid with trypsin ($p<0.01$) but pepsin after trypsin did not affect the detection ($p>0.05$) (Figure 4P). In general, around 85% of 5caC was co-existed with 5hmC (Figure 4P), but almost all 5hmC (98%) was co-localized with 5caC in HeLa cells (Figure 4Q). Both 5caC and 5hmC were mostly organized as diffuse pattern in the nuclei regardless of the type of antigen retrieval used (Figure 4R).

Co-localisation of 5caC and 5fC

In CF-1 cells, 5caC and 5fC was highly co-localized (more than 0.9) regardless of the use of antigen retrieval (Figure 5A-C). Similarly, almost all 5caC within the nucleus were co-localized with 5fC (Figure 5D), however trypsin treatment revealed a significant amount of 5fC (approximately 20%) that was not co-localized with 5caC ($p<0.05$ compared to acid alone, $p<0.01$ compared to the additional treatment with pepsin) (Figure 5E). 5caC and 5fC were mostly diffuse within the nucleus but some were localized in distinct focal regions (Figure 5F). In AR42J cells, trypsin alone ($p<0.0001$) and trypsin followed by pepsin ($p<0.001$) revealed less co-localization of 5caC with 5fC, but the average value was around 0.85 (Mander's and Pearson's correlations were similar to each other) (Figure 5G-I). Half of 5caC was found to co-localized with 5fC after sequential treatment of cells with acid, trypsin and pepsin compared to acid alone ($p<0.0001$) and with trypsin ($p<0.0001$) (Figure 5J) whereas almost all 5fC was co-localized with 5caC after any antigen retrieval application

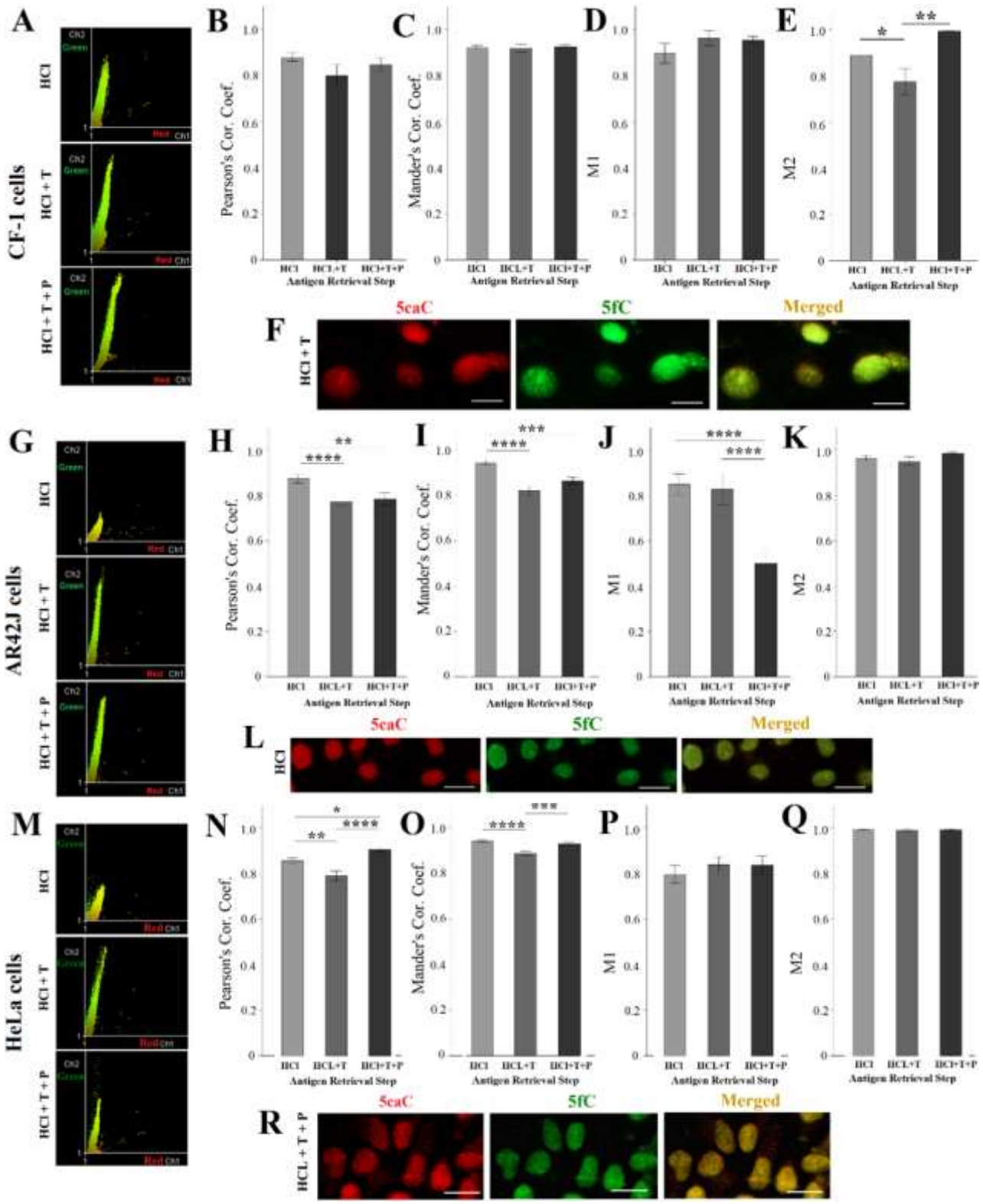

Figure 5. The co-localisation of 5caC and 5fC in CF-1, AR42J and HeLa cells**.** CF-1 cells **(A-F),** AR42J **(G-L)** and HeLa cells **(M-R)** include co-localisation dot plots of 5caC (red) and 5fC (green) after acid alone (HCl), acid + trypsin (HCl + T) and acid + trypsin + pepsin (HCl + T + P) **(A, G, M)**, bar graphs for the comparisons of Pearson's correlation coefficients **(B, H, N)**, Mander's correlation coefficients **(C, I, O)**, M1 values **(D, J, P)**, M2 values **(E, K, Q)** and representative microscopy images **(F, L, R)**. Bar graphs show +/- standard error of the mean of independent triplicates. Scale bar is 10 micron. $p<0.05$ (*), $p<0.01$ (**), $p<0.001$ (***) and $p<0.0001$ (****).

(Figure 5K). 5caC was diffusely localized but 5fC showed few focal accumulations within the nucleus (Figure 5L). HeLa cells showed a similar co-localization pattern with AR42J cells as the use of trypsin significantly provided more independent localization of 5caC and 5fC from each other (p<0.0001 compared to acid alone, p<0.001 compared to acid, trypsin and pepsin) (Mander's and Pearson's correlations were similar to each other) (Figure 5M-O). Around 20% of 5caC was found to localize independent from 5fC (Figure 5P), but a negligible amount of 5fC (less than 1%) was independently localize from 5caC (Figure 5Q). Like the other cells, both modifications were mostly found in diffuse staining but some foci with 5fC accumulation were present within the nucleus (Figure 5R).

Discussion

This study attempted to understand the variety in the co-localization of 5'-carboxycytosine with 5'-methylcytosine and its other derivatives within the normal and cancer cells using a newly developed immunofluorescence protocol. Different antigenic retrieval methods were used to reveal whether there was diversity in the co-existence of cytosine modifications. Immunostaining is an advantageous method for *in situ* detection of DNA modifications; however, it has some technical limitations in terms of accessibility of DNA regions of interest. Antigen retrieval is a crucial step in immunostaining for DNA epitopes to remove protein content around DNA. The standard application for antigen retrieval of modified cytosines includes the treatment of permeabilized cells with hydrochloric acid (1-4N) [24-26]. Following acid treatment, the use of trypsin alone or its sequential use with pepsin were shown to enhance the staining level of cytosine modifications in normal and cancer cells [20-22]. Trypsin and pepsin are proteolytic enzymes which hydrolyze hydrophilic and hydrophobic residues of proteins, respectively. These enzymes were used to target a diversity of proteins to be removed around DNA. Chromatin is a complex structure that composed of histones and DNA. DNA is also associated with non-histone proteins and this increases complexity of spatial organization of DNA and proteins. Epigenetic modifications can exist in euchromatic and heterochromatic regions, and this pattern is highly dynamic depending on the cell type and the cellular activities [27-35]. The intra-nuclear location of cytosine modifications therefore can be associated with their functions. The lack of complete antigen retrieval is problematic in immunostaining for understanding the locations within nuclear compartments as well as for measurement of the levels of modifications. Although there is no antigen retrieval strategy ensuring the complete binding of each antibody for cytosine modifications, enzyme treatments after acid that enhanced the detectable level of these as previously shown [20] did reveal the different patterns of co-localization in this study. The co-pattern of these modifications can suggest the associative function of modifications or distinct localization can indicate specific function of modifications depending on cell type or/and under specific conditions within the cells. However, the limitations of the study include the necessity for the higher resolution for visualization through confocal microscopy.

The staining pattern of cytosine modifications can vary in cells and also in developmental stages. In this study, 5caC is co-localized with 5meC, 5hmC or 5fC at around 76-92 % range in the cells experienced (Table 2). Most of 5caC was found to co-exist with 5hmC in differentiated liver cells whereas it showed

Table 2. Summarised comparison of co-localisation of 5caC with 5meC, 5hmC and 5fC in different cells after various antigen retrieval

CELLS	Co-localisation with 5meC		Co-localisation with 5hmC		Co-localisation with 5fC	
	Mander's coefficient	***P***	**Mander's coefficient**	***P***	**Mander's coefficient**	***P***
CF-1	HCl – **0.90** ± 0.022 T – **0.68** ± 0.120 P – **0.58** ± 0.140 Ave: **0.76** ± 0.170	HCl vs T (↓) $p<0.01$ HCl vs P (↓) $p<0.01$	HCl – **0.85** ± 0.080 T – **0.91** ± 0.060 P – **0.93** ± 0.030 Ave: **0.89** ± 0.070	HCl vs T (↑) $p<0.01$ T vs P (↑) $p<0.01$	HCl – **0.92** ± 0.036 T – **0.92** ± 0.050 P – **0.92** ± 0.023 Ave: **0.92** ± 0.070	$p>0.05$
AR42J	HCl – **0.89** ± 0.042 T – **0.83** ± 0.041 P – **0.85** ± 0.073 Ave: **0.86** ± 0.06	HCl vs T (↓) $p<0.05$	HCl – **0.90** ± 0.044 T – **0.84** ± 0.060 P – **0.84** ± 0.080 Ave: **0.86** ± 0.06	HCl vs T (↓) $p<0.05$ HCl vs P (↓) $p<0.05$	HCl – **0.94** ± 0.040 T – **0.82** ± 0.080 P – **0.86** ± 0.050 Ave: **0.88** ± 0.080	HCl vs T (↓) $p<0.0001$ HCl vs P (↓) $p<0.001$
HeLa	N/A		HCl – **0.90** ± 0.048 T – **0.86** ± 0.044 P – **0.91** ± 0.330 Ave: **0.88** ± 0.050	HCl vs T (↓) $p<0.01$ T vs P (↑) $p<0.0001$	HCl – **0.95** ± 0.018 T – **0.89** ± 0.036 P – **0.93** ± 0.036 Ave: **0.92** ± 0.040	HCl vs T (↓) $p<0.0001$ T vs P (↑) $p<0.001$

HCl: hydrochloric acid, T: trypsin, P: pepsin, Ave: average, ↓ decrease, ↑ increase

distinct location in hepatic progenitor cells [36]. However, in embryonic stem cells 5caC was tend to co-localize with 5hmC more than with 5meC [37]. The level of co-existence decreased with brain development in the mouse [37]. 5caC and 5fC are mostly considered as temporary and unstable modifications of cytosines during stem cell development, but 5hmC is thought to be more persistent mark throughout the nucleus [37-39]. The amounts of 5caC, 5fC and 5hmC were shown to gradually decrease by each DNA replication in mouse embryos before implantation [17, 38]. Apart from the normal development process, the pattern of cytosine modifications has been also shown to be altered in cancer cells. In brain tumor cells, both 5hmC and 5caC were detected at significant levels and those were also co-localized within the nucleus, whereas HeLa cells were shown to not to have detectable 5caC signal [40] suggesting that 5hmC and 5caC can be the epigenetic hallmarks of tumors specifically developed from neural stem cells. However, this study used only standard acid treatment for antigenic retrieval of both markers. Additional enzyme treatments could enhance the staining performance. The amount of 5caC in HeLa cells was detectable after any of antigen retrieval [20], and the present study also confirms the presence of 5caC in HeLa cells. Trypsin did reveal more content of 5caC independently localized from 5hmC and 5fC in these cells (represented by decreased Mander's co-localization coefficients). In both HeLa and AR42J cells, the detectable pattern of co-existence of 5caC and 5fC was significantly changed after the treatments with enzymes (Table 2). A decrease in the co-localization of 5caC with 5meC was detected in normal cells after enzyme treatments compared to AR42J cancer cells. In contrast, 5caC's co-localization with 5fC was not affected by the use of different antigen retrievals in normal fibroblasts. However, pepsin treatment provided almost 40 % of independent 5caC location from 5meC in CF-1 normal fibroblast cells. Therefore, 5caC's localization within the nucleus highly depends on solvent-exposure of carboxymethylated cytosines in normal cells suggesting its existence along different chromatin regions with different sensitivity against acid and/or enzymes (Table 2). These results can indicate that the detection of immune-localization of DNA modifications highly depends on three-

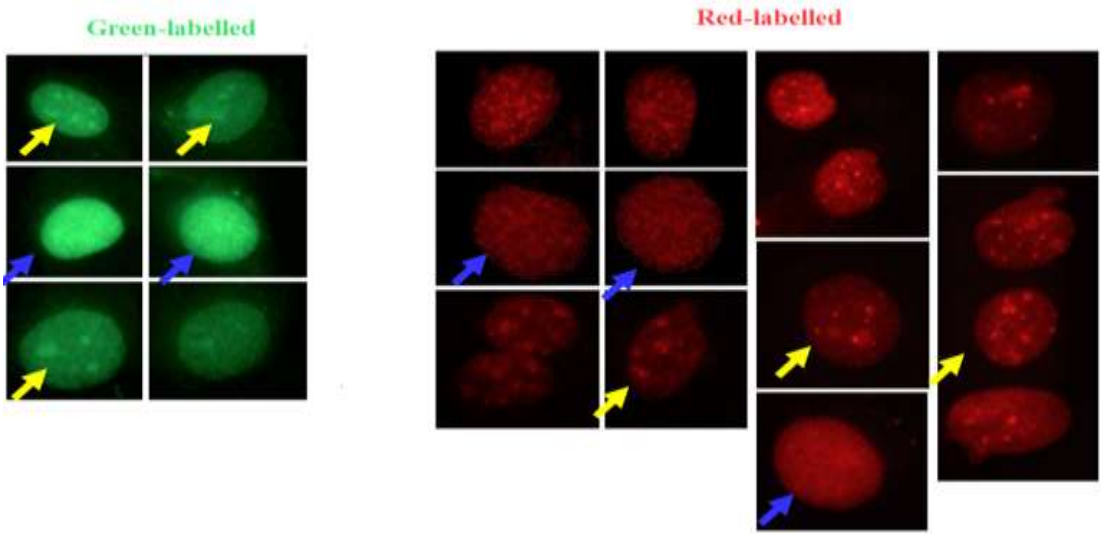

Figure 6. Staining pattern of 5caC after HCl and trypsin in CF-1 embryonic fibroblasts. CF-1 cells showed heterogeneity in 5caC staining as some cells had predominantly diffuse staining (blue arrows) but some had focal staining (yellow arrows).

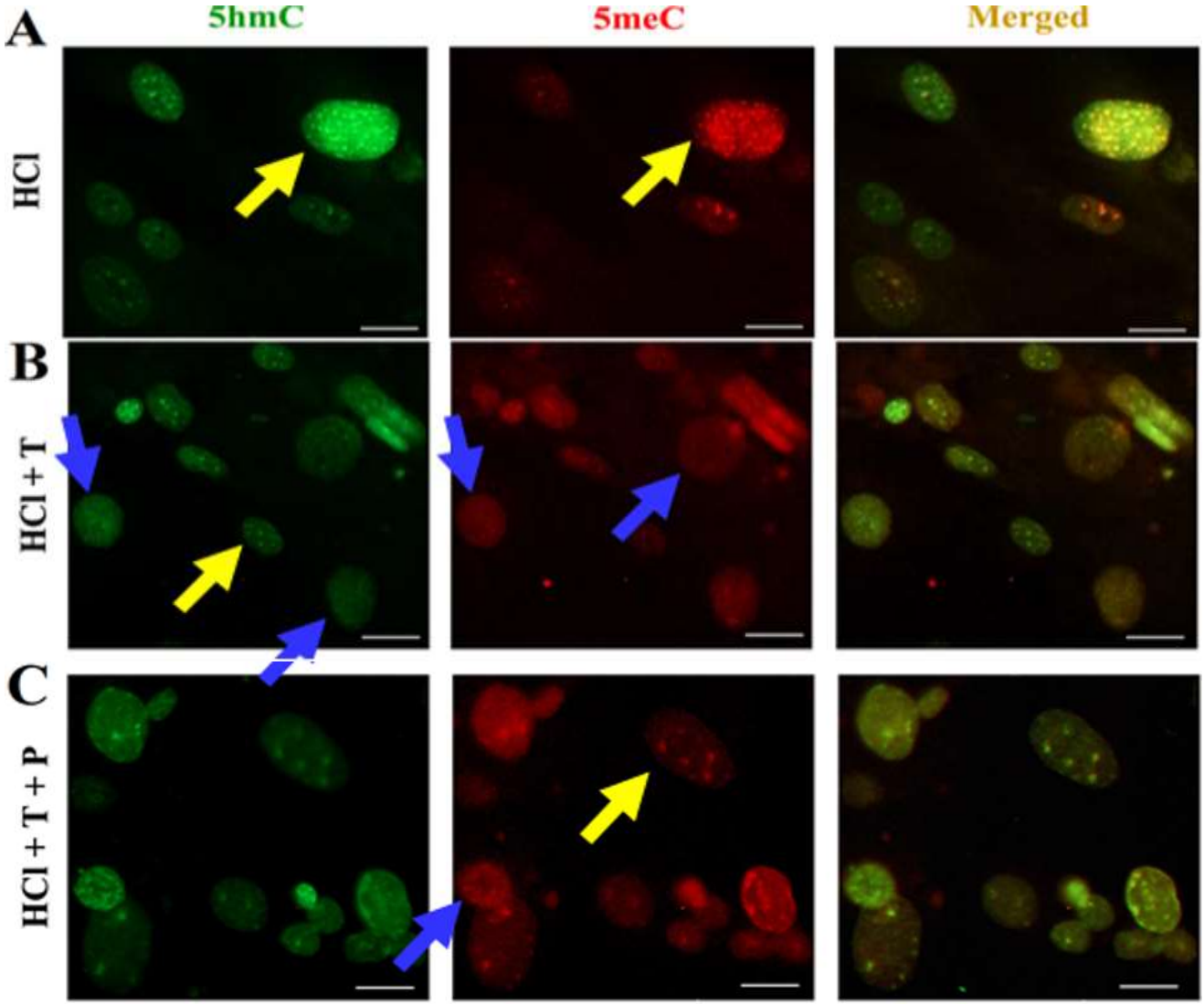

Figure 7. Staining pattern of 5meC and 5hmC in CF-1 cells after different antigen retrievals. CF-1 cells showed heterogeneity in 5meC and 5hmC staining as some cells had predominantly diffuse staining (blue arrows) but some had focal staining (yellow arrows).

dimensional structure of chromatin-DNA complex that is organized within the layers with different response to enzymatic reactions (Table 2). In general, compared to cancer cells, normal cells (mouse embryonic fibroblasts) showed more heterogenicity in terms of focal and/or diffuse staining of 5caC **(**Figure 6), 5hmC and 5meC (Figure 7).

Acknowledgements and Funding:

This study was supported by The Scientific and Technological Research Council of Turkey (TUBITAK) with the grant number 116Z733, and this study was also performed thanks to the equipment grant by Karadeniz Technical University (Grant Number: FAY-2015-141).

The author(s) received no financial support for the research, authorship, and/or publication of this article.

Conflict of Interest: *The authors declare that they have no conflict of interest.*

Ethical statement:

Ethics committee decision was not taken as it was a cell culture study.

References

[1]Pihlstrom L, Berge V, Rengmark A, et al. Parkinson's Disease Correlates With Promoter Methylation in the alpha-Synuclein Gene. Mov Disord. 2015; 30(4): 577-80.

[2]Ibn Sina A, Carrascosa L, Liang Z, et al. Epigenetically reprogrammed methylation landscape drives the DNA self-assembly and serves as a universal cancer biomarker. Nat Com. 2018;9(1):4915.

[3]Tang X, Ruan S, Tang Q, et al. DNA methylation profiles in the hippocampus of an Alzheimer's disease mouse model at mid-stage neurodegeneration. Int J Clin Exp Med. 2018; 11(11): 11876-88.

[4]Wu X, and Y Zhang, TET-mediated active DNA demethylation: mechanism, function and beyond. Nat Rev Genet. 2017; 18(9): 517-34.

[5]Sadakierska-Chudy A, Kostrzewa RM, Filip M. A comprehensive view of the epigenetic landscape part I: DNA methylation, passive and active DNA demethylation pathways and histone variants. Neurotox Res. 2015;27(1):84-97.

[6]He YF, Li BZ, Li Z, et al. Tet-Mediated Formation of 5-Carboxylcytosine and Its Excision by TDG in Mammalian DNA. Science. 2011; 333(6047): 1303-1307.

[7]Cortellino S, Xu J, Sannai M, et al. Thymine DNA Glycosylase Is Essential for Active DNA Demethylation by Linked Deamination-Base Excision Repair. Cell. 2011;146(1): 67-79.

[8]Ito S, Shen L, Dai Q, et al. Tet Proteins Can Convert 5-Methylcytosine to 5-Formylcytosine and 5-Carboxylcytosine. Science. 2011; 333(6047): 1300-1303.

[9]Wu H, D'alessio AC, Ito S, et al. Genome-wide analysis of 5-hydroxymethylcytosine distribution reveals its dual function in transcriptional regulation in mouse embryonic stem cells. Genes Dev. 2011;25(7): 679-84.

[10] Stroud H, Feng S, Kinney SM, et al. 5-Hydroxymethylcytosine is associated with enhancers and gene bodies in human embryonic stem cells. Genome Biol. 2011;12(6):R54.

[11] Iurlaro M, Ficz G, Oxley D, et al. A screen for hydroxymethylcytosine and formylcytosine binding proteins suggests functions in transcription and chromatin regulation. Genome Biol. 2013; 14(10):R119.

[12] Tao H, Xie P, Cao Y, et al. The Dynamic DNA Demethylation during Postnatal Neuronal Development and Neural Stem Cell Differentiation. Stem Cells Int. 2018; 2018: 2186301.

[13] Chamberlain A, Lin M, Lister RL, et al. DNA Methylation is Developmentally Regulated for Genes Essential for Cardiogenesis. J Am Heart Assoc. 2014; 19(3): e000976.

[14] Szulwach K, Li X, Li Y, et al. 5-hmC-mediated epigenetic dynamics during postnatal neurodevelopment and aging. Nat Neurosci. 2011; 14(12): 1607-16.

[15] Ruzov A, Tsenkina Y, Serio A, et al. Lineage-specific distribution of high levels of genomic 5-hydroxymethylcytosine in mammalian development. Cell Res. 2011; 21(9): 1332-42.

[16] Niles K, Chan D, La Selle S, et al. Critical Period of Nonpromoter DNA Methylation Acquisition during Prenatal Male Germ Cell Development. PloS One. 2011; 6(9): e24156.

[17] Inoue A, Shen L, Dai Q, et al. Generation and replication-dependent dilution of 5fC and 5caC during mouse preimplantation development. Cell Res. 2011;21(12):1670-76.

[18] Kinney SM, Chin HG, Vaisvila R, et al. Tissue-specific Distribution and Dynamic Changes of 5-Hydroxymethylcytosine in Mammalian Genomes. J Biol Chem. 2011; 286(28): 24685-93.

[19] Celik S, Y Li, O'Neill C. The Exit of Mouse Embryonic Fibroblasts from the Cell-Cycle Changes the Nature of Solvent Exposure of the 5 '-Methylcytosine Epitope within Chromatin. PloS One. 2014; 9(4): e92523.

[20] Celik-Uzuner S. Enhanced immunological detection of epigenetic modifications of DNA in healthy and cancerous cells by fluorescence microscopy. Microsc Res and Tech. 2019; 82(11):1962-72

[21] Li Y, O'Neill C. Persistance of Cytosine Methylation of DNA following Fertilisation in the Mouse. PloS One. 2012; 7(1): e30687.

[22] Li Y, and O'Neill C, 5'-methylcytosine and 5'-hydroxymethylcytosine Each Provide Epigenetic Information to the Mouse Zygote. PloS One, 2013; 8(5): e63689.

[23] Zinchuk V, Zinchuk O, and Okada T, Quantitative colocalization analysis of multicolor confocal immunofluorescence microscopy images: Pushing pixels to explore biological phenomena. Acta Histochem Cytochem. 2007; 40(4): 101-11.

[24] Ballestar E, Paz MF, Valle L, et al. Methyl-CpG binding proteins identify novel sites of epigenetic inactivation in human cancer. EMBO J. 2003; 22(23): 6335-45.

[25] Globisch D, Münzel M, Müller M, et al. Tissue Distribution of 5-Hydroxymethylcytosine and Search for Active Demethylation Intermediates. PloS One, 2010; 5(12): e15367.

[26] Lian CG, Xu Y, Ceol C, et al. Loss of 5-Hydroxymethylcytosine Is an Epigenetic Hallmark of Melanoma. Cell. 2012; 150(6): 1135-46.

[27] Alioui A, Wheldon LM, Abakir A, et al. 5-Carboxylcytosine is localized to euchromatic regions in the nuclei of

follicular cells in axolotl ovary. Nucleus. 2012; 3(6): 565-69.

[28] Cowell I, Papageorgiou N, Padget K, et al. Histone deacetylase inhibition redistributes topoisomerase IIβ from heterochromatin to euchromatin. Nucleus. 2011; 2(1): 61-71.

[29] Kang YK, Koo DB, Park JS, et al. Differential inheritance modes of DNA methylation between euchromatic and heterochromatic DNA sequences in ageing fetal bovine fibroblasts. FEBS Lett. 2001;498(1):1-5.

[30] Kubiura M, Okano M, Kimura H, et al. Chromosome-wide regulation of euchromatin-specific 5mC to 5hmC conversion in mouse ES cells and female human somatic cells. Chromosome Res. 2012;20(7):837-48.

[31] Papazvan R, Voronina E, Chapman JR, et al. Methylation of histone H3 at lysine 23 in meiotic heterochromatin. Epigenetics Chromatin. 2013; 6 (Suppl 1)(O13).

[32] Wen B, Wu H, Loh YH, et al. Euchromatin islands in large heterochromatin domains are enriched for CTCF binding and differentially DNA-methylated regions. BMC Genom. 2012; 13:566.

[33] Wongtawan T, Taylor JE, Lawson KA, et al. Histone H4K20me3 and HP1 alpha are late heterochromatin markers in development, but present in undifferentiated embryonic stem cells. J Cell Sci. 2011; 124(11): 1878-90.

[34] Chantalat S, Depaux A, Hery P, et al. Histone H3 trimethylation at lysine 36 is associated with constitutive and facultative heterochromatin. Genome Res. 2011;21(9):1426-37.

[35] Bernstein E, Duncan EM, Masui O, et al. Mouse polycomb proteins bind differentially to methylated histone H3 and RNA and are enriched in facultative heterochromatin. Mol Cell Biol. 2006; 26(7): 2560-69.

[36] Ramsawhook AH, Lewis LC, Eleftheriou M, et al. Immunostaining for DNA Modifications: Computational Analysis of Confocal Images. J Vis Exp. 2017;(127):56318.

[37] Wheldon LM, Abakir A, Ferjentsik Z, et al. Transient Accumulation of 5-Carboxylcytosine Indicates Involvement of Active Demethylation in Lineage Specification of Neural Stem Cells. Cell Rep. 2014; 7(5): 1353-61.

[38] Inoue A, and Zhang Y, Replication-Dependent Loss of 5-Hydroxymethylcytosine in Mouse Preimplantation Embryos. Science. 2011;334(6053):194.

[39] Iqbal K, Jin SG, Pfeifer GP, et al. Reprogramming of the paternal genome upon fertilization involves genome-wide oxidation of 5-methylcytosine. PNAS. 2011; 108(9): 3642-47.

[40] Ramsawhook A, Lewis L, Coyle B, et al. Medulloblastoma and ependymoma cells display increased levels of 5-carboxylcytosine and elevated TET1 expression. Clin Epigenetics. 2017; 9:18.

[41] Drohat AC, and Coey CT. Role of Base Excision "Repair" Enzymes in Erasing Epigenetic Marks from DNA. Chem Rev. 2016; 116(20): 12711-29.

[42] Santos F, Peat J, Burgess H, et al. Active demethylation in mouse zygotes involves cytosine deamination and base excision repair. Epigenetics Chromatin. 2013;6(1):39.